The nitrogen-fixing fern *Azolla* has a complex microbiome characterized by multiple modes of transmission

Michael J. Song[1,*], Fay-Wei Li[2], Forrest Freund[3], Carrie M. Tribble[4], Erin Toffelmier[5], Courtney Miller[5], H. Bradley Shaffer[5], and Carl J. Rothfels[6]

[1]*Department of Biology, Skyline College, San Bruno, CA 94066, USA*
[2]*Boyce Thompson Institute, Cornell University, Ithaca, NY 14853, USA*
[3]*Bureau of Land Management, USA*
[4]*School of Life Sciences, University of Hawai'i at Manoa, HI, United States; Current address: Department of Biology, University of Washington, Seattle, Washington*
[5]*Department of Ecology and Evolutionary Biology, University of California, Los Angeles, CA, USA; La Kretz Center for California Conservation Science, Institute for Environment and Sustainability, University of California, Los Angeles, CA 90095, USA*
[6]*Ecology Center and Department of Biology, Utah State University, Logan, UT 84322, USA*
[*]*corresponding author: songm@smccd.edu*

Abstract

Azolla is a floating fern that has closely evolved with a vertically transmitted obligate cyanobacterium endosymbiont—*Anabaena azollae*—that performs nitrogen fixation in specialized *Azolla* leaf pockets. This cyanobacterium has a greatly reduced genome and appears to be in the "advanced" stages of symbiosis, potentially evolving into a nitrogen-fixing organelle. However, there are also other lesser-known inhabitants of the leaf pocket whose role and mode of transmission are unknown. We sequenced 112 *Azolla* specimens collected across the state of California and characterized their metagenomes in order to identify the common bacterial endosymbionts of the leaf pocket and assess their patterns of co-diversification. Four taxa were found across all samples, establishing that there are multiple endosymbionts that consistently inhabit the *Azolla* leaf pocket. We found varying degrees of co-diversification across these taxa as well as varying degrees of isolation by distance and of pseudogenation, which implies that the endosymbiotic community is transmitted by a mix of horizontal and vertical mechanisms, and that some members of the microbiome are more facultative symbionts than others. These results show that the *Azolla* symbiotic community is complex, featuring members at potentially different stages of symbiosis evolution, further supporting the utility of the *Azolla* microcosm as a system for studying the evolution of symbioses.

Key Words: [*Azolla*, California Conservation Genomics Project, codiversification, coevolution, holobiont, microbiome, nitrogen-fixation, nitroplast, symbiosis]

Introduction

Azolla Lam. (Salviniaceae; Salviniales) is a genus of approximately nine species of floating ferns with specialized leaf pockets that house endosymbiotic bacteria. The most notable microbial inhabitant of the leaf pocket is *Anabaena azollae* (syn. *Nostoc azollae*, *Trichormus azollae*), which is a nitrogen-fixing cyanobacterium; the *Azolla-Anabaena* symbiosis can fix nitrogen at rates twice that of the legume-*Rhizobium* symbiosis (Watanabe, 1986; Beringer and Johnston, 1984), allowing, among other things, for *Azolla* populations to double their biomass in as little as two days (Peters et al., 1980). The *Anabaena* is vertically transmitted (Zheng et al., 2009) and shows near-perfect codiversification with its *Azolla* host (the *Anabaena* and *Azolla* phylogenies match each other; Li et al., 2018). In addition, the endosymbiont has a considerably reduced genome and can no longer live on its own (Ran et al., 2010; Li et al., 2018): it is potentially evolving into a nitrogen-fixing organelle, like the recently discovered nitroplast in some marine algae (Coale et al., 2024).

There are other known inhabitants of the leaf pocket in addition to the *Anabaena*, including members of the Rhizobiales, two novel species of which have been identified and found to perform denitrification and lack nitrogen fixation genes (Dijkhuizen et al., 2018), and potentially other cyanobacteria like *Fischerella* (Gunawardana and Pushpakumara, 2023). Other studies have further clarified that the *Azolla* microbiome is not only diverse, with many different bacteria having potential roles in promoting plant growth, but also exhibits substantial variation across host species (Banach et al., 2019; Yang et al., 2022). However, there is still no knowledge of the degree to which the members outside of *Anabaena azollae* have codiversified with the host, and, more generally, the degree to which the symbiotic community is a cohesive entity or an idiosyncratic assemblage of largely independent taxa.

A powerful tool for understanding novel associations is examining codiversification (Janz, 2011) between individual endosymbionts and a host. By assessing co-phylogenies and geographic patterns, we can infer whether the members of the core microbiome are mostly obligate or mostly facultative, which will give us a better understanding of the ecosystem within the leaf pocket. In particular, the leaf pocket provides an opportunity to study the evolution of symbioses by allowing glimpses of the process at different stages for different taxa–a spectrum that ranges from loose association and recruitment to intracellular endosymbiosis, such as the chloroplast or nitroplast which represents the far end of this spectrum Coale et al. (2024).

Here, we characterize the metagenome of *Azolla* and assess patterns of co-diversification across the common bacterial endosymbionts, using a large resequencing dataset set generated as part of the California Conservation Genomics Project.

Methods

Sample collection and sequencing

Field collections and identification

A total of one hundred and twelve samples of *Azolla* were collected (Supplemental Table 1) across the state of California as a part of the California Conservation Genome Project (CCGP; Shaffer et al., 2022). Potential collection sites were identified using the California Consortium of Herbaria Consortium of California Herbaria (2023) and iNaturalist (iNaturalist, 2023). Results were screened for georeferenced observations made after 2016 that included photographs to confirm the *Azolla* identification.

At each field site, the population was photo-documented at the habitat level and the super-macro level using a Canon PowerShot SX20 IS (Canon, Huntington, New York, USA) and the geographic coordinates were recorded with a Garmin inReach (Garmin Ltd., Schaffhausen, Switzerland). No more than 5% of the total population was sampled, or no more than a 5cm x 5cm mat, whichever was smaller. For plants that were growing neustonically, a pool-skimmer net was used to collect plants away from the shore, in an effort to gather specimens that were relatively undamaged by shoreline wave action. Plants growing terrestrially were carefully removed from the substrate as a matt. All specimens were placed into small, sealable plastic containers and stored in a cooler with ice until they were processed. If collections were made from the same water body, they were taken from at least 1 km apart.

Surface sterilization

In order to remove any surface bacterial contaminants, we followed a modified version of the surface sterilization the protocol in Dijkhuizen et al. (2018). After the first treatment, each specimen was transferred to a second 15ml centrifuge tube, and vortexed on low speed three times successively for 1–2 seconds in 3–4ml deionized water. Following the rinse, each individual was surface-sterilized by placing it into a 15ml centrifuge tube with 3–4ml 10% bleach and vortexing on low speed for 3–4 seconds. Once surface sterilized, the specimens were rinsed as above, dried with kimwipes, and flash-frozen at -80°C until it was time to extract DNA.

DNA extraction and sequencing

Total genomic and symbiont DNA was extracted using using standard CTAB extraction protocols described in (Doyle and Doyle, 1987). After extractions were complete, DNA quality and quantity were checked using 1% Agarose gel eletrophoresis with 0.1% GelRed Nuclease Dye (Biotum Inc., Fremont CA, USA) and Qubit spectrometry (Thermo Fisher Scientific, Waltham, Massachusetts, U.S.).

Library preparation was performed by the QB3-Berkeley Functional Genomics Laboratory at UC Berkeley. DNA was fragmented with an S220 Focused-Ultrasonicator (Covaris), and libraries prepared using the KAPA Hyper Prep kit for DNA (Roche KK8504). Truncated universal stub adapters were ligated to DNA fragments, which were then extended via PCR using unique dual indexing primers into full length Illumina adapters. Library quality was checked on an AATI (now Agilent) Fragment Analyzer. Libraries were then transferred to the QB3-Berkeley Vincent J. Coates Genomics Sequencing Laboratory, also at UC Berkeley. Library molarity was measured via quantitative PCR with the KAPA Library Quantification Kit (Roche KK4824) on a BioRad CFX Connect thermal cycler. Libraries were then pooled by molarity and sequenced on an Illumina NovaSeq 6000 S4 flowcell for 2 x 150 cycles, targeting at least 10Gb per sample. Fastq files were generated and demultiplexed using Illumina bcl2fastq2 v2.20 and default settings, on a server running CentOS Linux 7. Whole genome resequencing was performed at an average read depth of around 10x (mean = 12.16x; standard deviation = 5.9; min = 3.6x; max = 44.3x).

Additionally, one reference sample (collection FF365) was sequenced using PacBio Hifi Sequencing (Hifi) producing long-read sequencing data (average depth = 65.56x). The HiFi SMRTbell library was constructed using the SMRTbell gDNA Sample Amplification Kit (Pacific Biosciences, Menlo Park, CA; Cat. no. 101-980-000) and the SMRTbell Express Template Prep Kit 2.0 (Pacific Biosciences; Cat. no. 100-938-900) according to the manufacturer's instructions. Approximately 10 kb sheared DNA by the Megaruptor 3 system (Diagenode, Belgium; Cat. no. B06010003) was used for removal of single-strand overhangs at 37C for 15 minutes, DNA damage repair at 37C for 30 minutes, end-repair and A-tailing at 20C for 30 minutes and 65C for 30 minutes, and ligation of overhang adapters at 20C for 60 minutes. To prepare for library amplification by PCR, the library was purified with ProNex beads (Promega, Madison, WI; Cat. no. NG2002) for two PCR amplification conditions at 15 cycles each then another ProNex bead purification. Purified amplified DNA from both reactions were pooled in equal mass quantities for another round of enzymatic steps that included DNA repair, end-repair/A-tailing, overhang adapter ligation, and purification with ProNex beads. The PippinHT system (Sage Science, Beverly, MA; Cat no. HPE7510) was used for SMRTbell library size selection to remove fragments $<$ 6–10 kb. The 10–11 kb average HiFi SMRTbell library was sequenced at UC Davis DNA Technologies Core (Davis, CA) using one 8M SMRT cell, Sequel II sequencing chemistry 2.0, and 30-hour movies each on a PacBio Sequel IIe sequencer.

All data generated by CCGP can be found in the NCBI SRA (PRJNA720569).

Metagenome assembly and binning

We mapped the HiFi reads from our reference-genome sample against the *Azolla filiculoides* genome (v1.2; Li et al., 2018) using `BWA` v0.7.17 (Li and Durbin, 2010); this *A. filiculoides* genome was sequenced from an axenic, symbiont-free strain. We then extracted the unmapped reads using `Samtools` v1.9 (Li et al., 2009). These unmapped reads, which we expect are from the metagenome, were then uploaded to the BugSeq pipeline (Fan et al., 2021) for long-read taxonomic classification

and metagenome binning (Supplemental Table 2). The fasta assemblies from the metagenome binning were used downstream as reference sequences for the leaf pocket microbial taxa. Bacterial genome annotation was performed using `Prokka` v1.14.6 using default parameters (Seemann, 2014) and genes involved in nitrogen metabolism were identified manually by looking for genes with "nitrogen" in the annotation. The `Prokka` annotations were used to assess pseudogenation using `Pseudofinder` v1.1.0 (Syberg-Olsen et al., 2022). Relative abundance of microbes in the resequencing samples was assessed using METAgenomic PHyLogenetic ANalysis for metagenomic taxonomic profiling using default parameters (`MetaPhlAn` 4.0.3; Blanco-Míguez et al., 2023).

Variant calling and phylogeny inference

Resequencing samples had Illumina adapters removed and were trimmed using `Trimmomatic` (v0.39, Bolger et al. (2014)) using the following parameters: LEADING:3 TRAILING:3 MINLEN:36. Samples were then mapped to the *Azolla filiculoides* genome (v1.2; Li et al., 2009) using `BWA` (0.7.17; Li and Durbin, 2010). `bcftools` (v1.9; Danecek et al., 2021) was used to create an mpileup for all the samples and to call variants. Variants were filtered to have a QUAL$\geq$30 and to remove multiallelic SNPs and indels, monomorphic SNPs, and SNPs in the close proximity of indels (–SnpGap 10). Reads that did not map to the *Azolla filiculoides* nuclear or chloroplast genome were then recovered and mapped to the metagenome assemblies from the BugSeq output: *Anabaena azollae*, *Rhizobium*, *Caulobacter*, *Bradyrhizobium*, and *Rhizobiaceae*. For each microbial taxon, an mpileup was created and variants were called using `bcftools` (v1.9, Danecek et al. (2021)) with the following additional parameter: –ploidy 1. Variants were then filtered to have a QUAL$\geq$30 and no monomorphic SNPs using `bcftools` (v1.9; Danecek et al., 2021).

Alignments of SNPs for the *Azolla* samples and for each of the five focal microbionts that were found in each sample (*Anabaena azollae*, *Rhizobium*, *Caulobacter*, *Bradyrhizobium*, and *Rhizobiaceae* sp. 2) were then created using the `phylo` command in `VCF-kit` (v0.2.9; Cook and Andersen, 2017)). For the *Azolla* alignment, heterozygous sites were excluded as per the recommended usage (Cook and Andersen, 2017). Maximum likelihood trees were then inferred for these taxa using `IQTree` (v1.6.12; Nguyen et al., 2015) under the GTR+ASC model, which accounts for the variable-only ascertainment bias in SNP datasets, and support values were estimated with the ultrafast bootstrap approximation (Minh et al., 2013; Hoang et al., 2018) with 1000 bootstrap replicates.

Assemblies and alignments of whole *Azolla* chloroplasts were produced using `GetOrganelle` v1.7.7.0 and `Homblocks`, both with default parameters (Bi et al., 2018; Jin et al., 2020). We included in this alignment all of the previously published *Azolla* chloroplast genomes (Genbank: MF177092.1, MF177091.1, ON684377.1, MF177090.1, MF177089.1, MF177088.1, MF177094.1, MF177093.1). From this alignment we inferred a tree using `IQTree` v1.6.12 under a GTR+I+G model with 1000 ultrafast bootstrap replicates (Nguyen et al., 2015).

We also used a coalescent-based approach, since we expect incongruence due to our intraspecific sampling (Supplemental Figure 4). Trees were inferred from the *Azolla* nuclear SNP alignment described above using `SVDquartets` (Chifman and Kubatko, 2014) implemented in `PAUP*` (v4.0; Swofford, 2003). One hundred bootstrap replicates were performed with quartet sampling of 100,000 quartets. We then made a majority rule consensus tree from the bootstrap trees and resolved polytomies randomly for downstream analysis that require bifurcating trees using the "fix.poly" function in the `RRphylo` package in `R` (Castiglione et al., 2018).

Codiversification and spatial analyses

Codiversification analyses and data visualization was performed using `R` (R Core Team et al., 2013) with the packages `ape` (Paradis et al., 2004) and `phytools` (Revell, 2012). For the plastome tree, we rooted the tree with *Azolla nilotica*. The other trees were visualized using midpoint rooting since they are unrooted; this orientation resulted in two major clades—*A. filiculoides* + *A. rubra* on one side and *A. caroliniana, A. microphylla*, and allies on the other—consistent with the results of studies that applied outgroup rooting (*e.g.*, Li et al., 2018; Metzgar et al., 2007; Madeira et al., 2013). Statistical tests of codiversification were performed between two trees based on tree distance for both RF (Robinson and Foulds, 1981) and SPR (Swofford, 1990) distances using the "cospeciation" function in `phytools`. P-values were calculated both by simulation of pure-birth trees and by permutation of tip labels on a fixed tree. Five hundred simulations (and 500 permutations) were performed for each test of the null hypothesis that there are no similarity between trees. Another statistical test of codiversification was performed using the "parafit" function (described in Legendre et al., 2002) in `ape` using the default parameters and 999 permutations.

The spatial distribution of the taxa was visualized using `R` and the packages `phytools` (Revell, 2012) and `maps` (code by Richard A. Becker et al., 2021). A Mantel test based on Spearman's rank correlation rho was performed with 9999 permutations using the `vegan` package in `R` in order to test for isolation by distance (Oksanen et al., 2022).

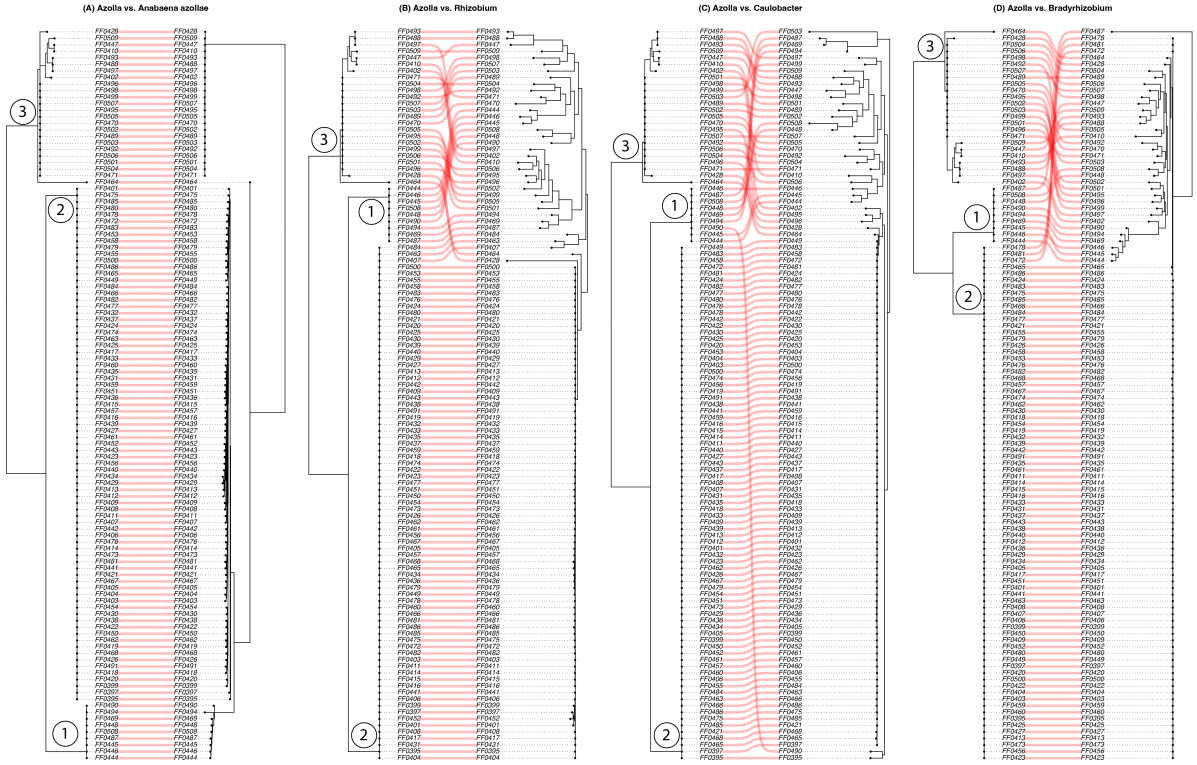

Figure 1: Co-phylogenies in order from left to right: *Azolla* and *Anabaena azollae*, *Azolla* and *Rhizobium*, *Azolla* and *Caulobacter*, and *Azolla* and *Bradyrhizobium*. All *Azolla* phylogenies are from the plastome data.

.

Table 1: Testing for isolation by distance. Mantel statistics based on Spearman's rank correlation rho, permutations = 9999

Taxon	Mantel statistic r	Significance
Anabaena azollae	0.2462	1.00E-04
Rhizobium	0.2271	0.0017
Caulobacter	0.3791	1.00E-04
Bradyrhizobium	-0.04252	0.7271
Azolla Plastome Tree	-0.1013	0.9679

Results

Characterization of the *Azolla* leaf pocket metagenome

From the reference-genome HiFi data, the BugSeq pipeline assembled 30 unique metagenomic bins ranging from 7.1 Kbp to 5,361.4 Kbp with N50 scores ranging from 7.1 to 1,079.5 Kbp (Supplemental Table 2). Five of these putative bacterial genomes were found in all of our samples. Two of these genomes were nearly complete according to BUSCO scores using the default BugSeq pipeline datasets (Simão et al., 2015; Fan et al., 2021): *Anabaena azollae* and *Rhizobium* sp. Genomes with mapped reads from every sample were included for downstream analysis. These included *Anabaena azollae* (53.6%), *Rhizobium* sp. (1.7%), *Bradyrhizobium* sp. (0.2%), *Caulobacter* sp. (0.2%) and a member of Rhizobiaceae species 2 (0.2%). When comparing the phylogenies inferred from SNP data, we found that the trees of *Rhizobium* sp. and Rhizobiaceae sp. 2 were essentially identical, implying that they are the same taxon and therefore, only *Rhizobium* sp. was analysed in the later analyses.

The `prokka` annotation found six nitrogen fixation (nif) coding sequences in *Anabaena azollae* and none in *Caulobacter* sp., *Rhizobium* sp., or *Bradyrhizobium* sp. Two *nar* nitrate reductase coding sequences were found in *Anabaena azollae* and none in *Caulobacter* sp., *Rhizobium* sp., or *Bradyrhizobium* sp. No *nir* nitrite reductase or *nos* nitrous oxide reductase coding sequences were found in any of the assemblies.

The `Pseudofinder` analysis revealed that there is some pseudogenization occuring across all of the common microbiome members. In the main endosymbiont, 32.4% of genes were found to be pseudogenized; *Rhizobium* sp. was found to have 5.6% of genes pseudogenized, *Bradyrhizobium* sp. 6.3%, and *Caulobacter* sp. 5.8%.

The `MetaPhlAn` taxonomic profiling of samples revealed that the vast majority of reads were of the main endosymbiont cyanobacterium (average across all sam-

ples = 94.89%, Supplemental Figure 2) followed by Proteobacteria (4.6%). However, for two samples (FF0505, FF0489) *Anabaena azollae* was not found to be at the highest abundance, possibly due to contamination or disease. A diverse group of phyla were found at much lower abundances, including: Actinobacteria, Armatimonadetes, Bacteroidetes, Chloroflexi, Cyanobacteria, Firmicutes, Gemmatimonadetes, Nitrospirae, Planctomycetes, Proteobacteria, Spirochaetes, Verrucomicrobia, as well as unclassified bacteria.

Azolla phylogenies

Phylogenies inferred from the plastome sequences (Supplemental Fig. 1), the concatenated nuclear SNPs (Supplemental Fig. 3), and the nuclear "species tree" inferred with SVDquartets (Supplemental Figure 4) were all congruent. For simplicity, and to avoid any complications due to coalescent variance, we focus downstream analyses on the plastome phylogeny. Most distantly related to the other samples is a clade corresponding to *A. filiculoides* (Clade 3, Figure 1). This *A. filiculoides* group has surprisingly very long branch lengths on the concatenated-SNP tree (Supplemental Fig. 3). Our other samples fall in two clades, the largest of which (Clade 2, Figure 1) includes reference sequences of *A. caroliniana* and the smaller of which (Clade 1, Figure 1) is sister to (but divergent from) published plastomes of *A. mexicana/microphylla* (Supplemental Fig. 1; a putative *A. pinnata* sequence that falls in this last clade is an "UNVERIFIED" sequence on Genbank that is almost certainly misidentified—*Azolla pinnata* belongs to a different subgenus and is only distantly related to the taxa in this study).

Codiversification of endosymbionts

Azolla and its symbionts have varying degrees of co-diversification (Figure 1). *Azolla* and its main endosymbiont *Anabaena azollae* exhibit strong co-diversification, as expected, with three major clades found in each. The other focal symbionts are inferred to have a large major clade that is associated with the Clade 2 in the *Azolla* phylogeny, but with more variation and longer branches in the other more distantly related groups.

The *Azolla* and *Anabaena azollae* trees significantly exhibited co-diversification across four of the five tests (Supplemental Table 3). Similarly, *Rhizobium* sp. also exhibited a strong signal of co-diversification with the plastome tree (4/5 tests significant). The other two taxa (*Caulobacter* sp. and *Bradyrhizobium* sp.) exhibited some signal of co-diversification: 3/5 and 2/5 tests significant, respectively.

The endosymbiont phylogenies also had significant associations with other endosymbionts. *Caulobacter* sp. was found to be significantly associated with *Bradyrhizobium* sp. across all tests and with *Rhizobium* sp. across four of the five tests. *Bradyrhizobium* sp. was found to be significantly associated with with *Rhizobium* sp. in two tests, and *Anabaena azollae* with *Caulobacter* sp. in two tests and with *Bradyrhizobium* sp. in one test.

Geographic Patterns

Clades 1 and 2 (red in Supplemental Fig. 5) are generally associated with northern samples and Clade 3 (blue in Supplemental Fig. 5) is frequently southern, although these patterns are not consistent (Supplemental Figure 5). Despite these trends, we cannot reject the null hypothesis that there is no relationship between genetic and geographic distances for *Azolla* (Table 1). This is likewise the case for *Bradyrhizobium*. However for *Anabaena azollae*, *Caulobacter* sp., and *Rhizobium* sp., there is a significant correlation between the geographic and phylogenetic distance matrices for each taxon, which implies isolation by distance for these groups (Table 1).

Discussion

Azolla diversity in California

The diversity of *Azolla* in California is often treated under two species: *Azolla filiculoides* Lam. and a second taxon treated as either *Azolla microphylla* Kaulf. or *A. mexicana* C.Presl. (Jepson eFlora, 2020; Flora of North America Editorial Committee, 1993). In addition, the potentially invasive *A. pinnata* has been recently reported from the state (Song et al., 2023). Our results highlight the need for further study of the taxonomic diversity of *Azolla* in California, as we find at least three major clades (within subgenus *Azolla*—*A. pinnata*, in subgenus *Rhizosperma*, is outside our taxonomic scope). Of these three clades, one is fairly confidently attributable to *A. filiculoides* (Supplemental Fig. 1). However, the identity of members of the other two clades is unclear. Surprisingly, neither clade appears to correspond to *A. microphylla/A. mexicana*; apparently, despite our expectation that this would be the most common taxon in California, it was absent from our sample. Instead Clade 1, sister to the *A. microphylla/mexicana* reference sequences, includes samples from eastern North America, and likely corresponds to the taxon usually treated as *A. caroliniana*. If these plants are indeed *A. caroliniana*, that would be a remarkable extension to the known range of that species, which is currently understood to be restricted to eastern North America (Flora of North America Editorial Committee, 1993). Clade 2—comprising 77 of our 112 samples—is even more enigmatic: it is sister to Clade 1 + *A. microphylla/mexicana*, and also corresponds to the taxon usually treated as *A. car-*

oliniana. Further analysis of just the plastid *trnGR* region, places these sequences within a group containing the lineage Madeira et al. (2013) refer to as an undescribed "*A.* species". However, a thorough examination of the type specimens and other data will be necessary to confidently attach names to these lineages; this work, and a broader taxonomic revision of *Azolla*, is not within the scope of this paper, but our findings should encourage a thorough reassessment of the group in California given the new genomic resources available.

The *Azolla* symbiotic community

While dominated by its main endosymbiont, we found three other major endosymbiont taxa in the *Azolla* leaf pocket. *Bradyrhizobium* sp. and *Rhizobium* sp. are both members of Rhizobiales, corroborating the results of Dijkhuizen et al. (2018) who found two major Rhizobiales taxa in the *Azolla filiculoides* leaf pocket. The other member, *Caulobacter* sp., is a well-known and common bacterium in freshwater systems, although it can be found in diverse environments (Wilhelm, 2018). These four taxa were found in every one of the 112 samples. Importantly, we found that all of these non *Anabaena azollae* members exhibit pseudogenization of around 5% of their genes; *Anabaena azollae*, on the other hand, had around 30% of its genes pseudogenized. This high degree of pseudogenization is similar to the main endosymbiont in *Azolla filiculoides*, which is also around 30% pseudogenized (Ran et al., 2010). To put this into context, the normal amount of pseudogenization for non-endosymbiotic bacteria is zero, such as was found in other free-living members of Nostocales (Ran et al., 2010).

When we assessed the phylogenies for co-diversification, we found strong evidence that *Anabaena azollae* is co-evolving with *Azolla*, which is what we expected due to its vertical transmittance (Ran et al., 2010; Li et al., 2018) and underscores the efficacy of this approach. When we assessed the other taxa, we found that there is some signal for co-diversification between *Azolla* and *Rhizobium* sp., *Bradyrhizobium* sp. and *Caulobacter* sp. We also found that the phylogenies of the endosymbionts were associated with each other and hypothesized that this was due to shared patterns of isolation by distance. When we tested for this, we found that the ML plastome tree did not exhibit a pattern of isolation by distance. For the bacterial taxa, all but *Bradyrhizobium* exhibited patterns of isolation by distance.

If everything in the leaf pocket were to be vertically transmitted like *Anabaena azollae*, then all of the phylogenies should mirror that of the host. If nothing is being vertically transmitted, we expect to find random patterns between the endosymbiont and the host and patterns that are geographic. We do not find evidence for either of those scenarios, but rather an intermediate between them, which implies that there is some horizontal transmission as well as some vertical transmission occurring. While the limitations of Mantel tests are well known (Bradburd et al., 2013), this pattern is supported by the additional evidence that these taxa were consistently found in every single sample, they all exhibit considerable degrees of pseudogenation, and that they do not exhibit strong co-diversification with the host.

One potential hypothesis for why there is a consistent core microbiome but only loose patterns of co-diversification, could be that some bacteria are able to be consistently recruited (maybe by interfacing with the well characterized ammonium and sucrose exchange; Eily et al., 2019), while others end up in the leaf pocket as a general refugium for bacteria (de Vries and de Vries, 2022). Then once in the leaf pocket, microbes may find themselves being transmitted vertically with the host, but in the absence of strong selection for them, they also may find themselves outcompeted and displaced by similar taxa that invade or that the host also recruits from the environment, only to be picked up again later on.

Even though these were partial genome assemblies and so we were unable to assess all of the genes that these endosymbionts have and metabolic roles that they play, the possibility remains that some taxa have evolved to be freeloaders off of the *Anabaena* nitrogen-fixation symbiosis and its associated metabolic products and may even be in conflict with *Anabaena* (Dijkhuizen et al., 2018). The taxonomy and function of these endosymbionts should be investigated in more depth in the future in order to understand what functions and roles these taxa may play in the leaf pocket, if at all. For example, the symbionts may be in metabolic collaboration, competition, or there may be Black Queen processes operating whereby there is a division of labor (Koskella and Bergelson, 2020; Morris et al., 2012). Future work should attempt to get full length assemblies of these bacterial genomes to assess genome reduction as an additional line of evidence for the differences between these putatively obligate and facultative members of the microbiome.

Author Contributions

M.J.S, F-W.L., F.F., E.T., C.M., B.S., and C.J.R designed and executed the experiment. M.J.S performed the analyses. M.J.S, F-W.L., F.F., E.T., C.M., B.S., C.M.T. and C.J.R contributed with the manuscript.

Acknowledgements

We would like to thank Britt Koskella for her discussion and insights.

Data accessibility

All data generated by CCGP can be found in the NCBI SRA (PRJNA720569).

Supplemental Tables and Figures

List of Supplemental Tables:

Supplemental Table 1. Sample collection data for this study.

List of Supplemental Figures:

Supplemental Figure 2. Violin plots of the relative abundance of the two most abundant phyla across all samples with the mean and standard deviation in red.

Supplemental Figure 3. ML phylogeny of *Azolla* samples inferred from SNP data with bootstrap values at nodes and branch length units in nucleotide substitutions per site.

Supplemental Figure 4. Coalescent tree inferred using SVDQuartets with bootstrap values at nodes and branch lengths in coalescent units.

References

Banach, A., Kuźniar, A., Mencfel, R., and Wolińska, A. (2019). The study on the cultivable microbiome of the aquatic fern azolla filiculoides l. as new source of beneficial microorganisms. *Applied Sciences*, 9(10):2143.

Beringer, J. E. and Johnston, A. W. (1984). The significance of symbiotic nitrogen fixation in plant production. *Critical reviews in plant sciences*, 1(4):269–286.

Bi, G., Mao, Y., Xing, Q., and Cao, M. (2018). Homblocks: a multiple-alignment construction pipeline for organelle phylogenomics based on locally collinear block searching. *Genomics*, 110(1):18–22.

Blanco-Míguez, A., Beghini, F., Cumbo, F., McIver, L. J., Thompson, K. N., Zolfo, M., Manghi, P., Dubois, L., Huang, K. D., Thomas, A. M., et al. (2023). Extending and improving metagenomic taxonomic profiling with uncharacterized species using metaphlan 4. *Nature Biotechnology*, pages 1–12.

Bolger, A. M., Lohse, M., and Usadel, B. (2014). Trimmomatic: a flexible trimmer for illumina sequence data. *Bioinformatics*, 30(15):2114–2120.

Bradburd, G. S., Ralph, P. L., and Coop, G. M. (2013). Disentangling the effects of geographic and ecological isolation on genetic differentiation. *Evolution*, 67(11):3258–3273.

Castiglione, S., Tesone, G., Piccolo, M., Melchionna, M., Mondanaro, A., Serio, C., Di Febbraro, M., and Raia, P. (2018). A new method for testing evolutionary rate variation and shifts in phenotypic evolution. *Methods in Ecology and Evolution*, 9(4):974–983.

Chifman, J. and Kubatko, L. (2014). Quartet inference from snp data under the coalescent model. *Bioinformatics*, 30(23):3317–3324.

Coale, T. H., Loconte, V., Turk-Kubo, K. A., Vanslembrouck, B., Mak, W. K. E., Cheung, S., Ekman, A., Chen, J.-H., Hagino, K., Takano, Y., et al. (2024). Nitrogen-fixing organelle in a marine alga. *Science*, 384(6692):217–222.

code by Richard A. Becker, O. S., version by Ray Brownrigg. Enhancements by Thomas P Minka, A. R. W. R., and Deckmyn., A. (2021). *maps: Draw Geographical Maps*. R package version 3.4.0.

Consortium of California Herbaria (2023). University of California and Jepson Herbaria. `https://ucjeps.berkeley.edu/consortium/`. Accessed Mar 3rd, 2023.

Cook, D. E. and Andersen, E. C. (2017). Vcf-kit: assorted utilities for the variant call format. *Bioinformatics*, 33(10):1581–1582.

Danecek, P., Bonfield, J. K., Liddle, J., Marshall, J., Ohan, V., Pollard, M. O., Whitwham, A., Keane, T., McCarthy, S. A., Davies, R. M., et al. (2021). Twelve years of samtools and bcftools. *Gigascience*, 10(2):giab008.

de Vries, S. and de Vries, J. (2022). Evolutionary genomic insights into cyanobacterial symbioses in plants. *Quantitative Plant Biology*, 3:e16.

Dijkhuizen, L. W., Brouwer, P., Bolhuis, H., Reichart, G.-J., Koppers, N., Huettel, B., Bolger, A. M., Li, F.-W., Cheng, S., Liu, X., et al. (2018). Is there foul play in the leaf pocket? the metagenome of floating fern azolla reveals endophytes that do not fix n2 but may denitrify. *New Phytologist*, 217(1):453–466.

Doyle, J. J. and Doyle, J. L. (1987). A rapid dna isolation procedure for small quantities of fresh leaf tissue. *Phytochemical bulletin*.

Eily, A. N., Pryer, K. M., and Li, F.-W. (2019). A first glimpse at genes important to the azolla–nostoc symbiosis. *Symbiosis*, 78:149–162.

Fan, J., Huang, S., and Chorlton, S. D. (2021). Bugseq: a highly accurate cloud platform for long-read metagenomic analyses. *BMC bioinformatics*, 22:1–12.

Flora of North America Editorial Committee, e. (1993). *Flora of North America: Volume 2: Pteridophytes and Gymnosperms*, volume 2. Oxford University Press.

Gunawardana, D. and Pushpakumara, B. U. (2023). Molecular characterization of fischerella uthpalarensis, the first subsection v cyanobiont from a tropical azolla species containing dual nitrogenases. *bioRxiv*, pages 2023–03.

Hoang, D. T., Chernomor, O., Von Haeseler, A., Minh, B. Q., and Vinh, L. S. (2018). Ufboot2: improving the ultrafast bootstrap approximation. *Molecular biology and evolution*, 35(2):518–522.

iNaturalist (2023). `https://www.inaturalist.org/`. Accessed Mar 3rd, 2023.

Janz, N. (2011). Ehrlich and raven revisited: mechanisms underlying codiversification of plants and enemies. *Annual review of ecology, evolution, and systematics*, 42:71–89.

Jepson eFlora (2020). Jepson eflora project.

Jin, J.-J., Yu, W.-B., Yang, J.-B., Song, Y., DePamphilis, C. W., Yi, T.-S., and Li, D.-Z. (2020). Getorganelle: a fast and versatile toolkit for accurate de novo assembly of organelle genomes. *Genome biology*, 21:1–31.

Koskella, B. and Bergelson, J. (2020). The study of host–microbiome (co) evolution across levels of selection. *Philosophical Transactions of the Royal Society B*, 375(1808):20190604.

Legendre, P., Desdevises, Y., and Bazin, E. (2002). A statistical test for host–parasite coevolution. *Systematic biology*, 51(2):217–234.

Li, F.-W., Brouwer, P., Carretero-Paulet, L., Cheng, S., De Vries, J., Delaux, P.-M., Eily, A., Koppers, N., Kuo, L.-Y., Li, Z., et al. (2018). Fern genomes elucidate land plant evolution and cyanobacterial symbioses. *Nature plants*, 4(7):460–472.

Li, H. and Durbin, R. (2010). Fast and accurate long-read alignment with burrows–wheeler transform. *Bioinformatics*, 26(5):589–595.

Li, H., Handsaker, B., Wysoker, A., Fennell, T., Ruan, J., Homer, N., Marth, G., Abecasis, G., Durbin, R., and Subgroup, . G. P. D. P. (2009). The sequence alignment/map format and samtools. *bioinformatics*, 25(16):2078–2079.

Madeira, P. T., Center, T. D., Coetzee, J. A., Pemberton, R. W., Purcell, M. F., and Hill, M. P. (2013). Identity and origins of introduced and native *Azolla* species in Florida. *Aquatic botany*, 111:9–15.

Metzgar, J. S., Schneider, H., and Pryer, K. M. (2007). Phylogeny and divergence time estimates for the fern genus *Azolla* (Salviniaceae). *International Journal of Plant Sciences*, 168(7):1045–1053.

Minh, B. Q., Nguyen, M. A. T., and Von Haeseler, A. (2013). Ultrafast approximation for phylogenetic bootstrap. *Molecular biology and evolution*, 30(5):1188–1195.

Morris, J. J., Lenski, R. E., and Zinser, E. R. (2012). The black queen hypothesis: evolution of dependencies through adaptive gene loss. *MBio*, 3(2):e00036–12.

Nguyen, L.-T., Schmidt, H. A., Von Haeseler, A., and Minh, B. Q. (2015). Iq-tree: a fast and effective stochastic algorithm for estimating maximum-likelihood phylogenies. *Molecular biology and evolution*, 32(1):268–274.

Oksanen, J., Simpson, G. L., Blanchet, F. G., Kindt, R., Legendre, P., Minchin, P. R., O'Hara, R., Solymos, P., Stevens, M. H. H., Szoecs, E., Wagner, H., Barbour, M., Bedward, M., Bolker, B., Borcard, D., Carvalho, G., Chirico, M., De Caceres, M., Durand, S., Evangelista, H. B. A., FitzJohn, R., Friendly, M., Furneaux, B., Hannigan, G., Hill, M. O., Lahti, L., McGlinn, D., Ouellette, M.-H., Ribeiro Cunha, E., Smith, T., Stier, A., Ter Braak, C. J., and Weedon, J. (2022). *vegan: Community Ecology Package*. R package version 2.6-4.

Paradis, E., Claude, J., and Strimmer, K. (2004). Ape: analyses of phylogenetics and evolution in r language. *Bioinformatics*, 20(2):289–290.

Peters, G. A., Toia Jr, R. E., Evans, W. R., Crist, D. K., Mayne, B. C., and Poole, R. E. (1980). Characterization and comparisons of five n2-fixing azolla-anabaena associations, i. optimization of growth conditions for biomass increase and n content in a controlled environment. *Plant, Cell & Environment*, 3(4):261–269.

R Core Team, R. et al. (2013). R: A language and environment for statistical computing.

Ran, L., Larsson, J., Vigil-Stenman, T., Nylander, J. A., Ininbergs, K., Zheng, W.-W., Lapidus, A., Lowry, S., Haselkorn, R., and Bergman, B. (2010). Genome erosion in a nitrogen-fixing vertically transmitted endosymbiotic multicellular cyanobacterium. *PLoS One*, 5(7):e11486.

Revell, L. J. (2012). phytools: an r package for phylogenetic comparative biology (and other things). *Methods in ecology and evolution*, (2):217–223.

Robinson, D. F. and Foulds, L. R. (1981). Comparison of phylogenetic trees. *Mathematical biosciences*, 53(1-2):131–147.

Seemann, T. (2014). Prokka: rapid prokaryotic genome annotation. *Bioinformatics*, 30(14):2068–2069.

Shaffer, H. B., Toffelmier, E., Corbett-Detig, R. B., Escalona, M., Erickson, B., Fiedler, P., Gold, M., Harrigan, R. J., Hodges, S., Luckau, T. K., et al. (2022). Landscape genomics to enable conservation actions: the california conservation genomics project. *Journal of Heredity*, 113(6):577–588.

Simão, F. A., Waterhouse, R. M., Ioannidis, P., Kriventseva, E. V., and Zdobnov, E. M. (2015). Busco: assessing genome assembly and annotation completeness with single-copy orthologs. *Bioinformatics*, 31(19):3210–3212.

Song, M. J., Huynh, M., Lahmeyer, S., and Sedaghatpour, M. (2023). First record of the invasive *Azolla pinnata* subsp. *pinnata* (Salviniaceae) in California. *American Fern Journal*, 113(1):56–57.

Swofford, D. L. (1990). Phylogenetic reconstruction. *Molecular systematics*, pages 411–501.

Swofford, D. L. (2003). Paupˆ* phylogenetic analysis using parsimony (ˆ* and other methods). version 4. *http://paup. csit. fsu. edu/*.

Syberg-Olsen, M. J., Garber, A. I., Keeling, P. J., McCutcheon, J. P., and Husnik, F. (2022). Pseudofinder: detection of pseudogenes in prokaryotic genomes. *Molecular biology and evolution*, 39(7):msac153.

Watanabe, I. (1986). Nitrogen fixation by non-legumes in tropical agriculture with special reference to wetland rice. *Plant and Soil*, 90:343–357.

Wilhelm, R. C. (2018). Following the terrestrial tracks of caulobacter-redefining the ecology of a reputed aquatic oligotroph. *The ISME journal*, 12(12):3025–3037.

Yang, Y.-Q., Deng, S.-F., Yang, Y.-Q., and Ying, Z.-Y. (2022). Comparative analysis of the endophytic bacteria inhabiting the phyllosphere of aquatic fern azolla species by high-throughput sequencing. *BMC microbiology*, 22(1):1–11.

Zheng, W., Bergman, B., Chen, B., Zheng, S., Xiang, G., and Rasmussen, U. (2009). Cellular responses in the cyanobacterial symbiont during its vertical transfer between plant generations in the azolla microphylla symbiosis. *New Phytologist*, 181(1):53–61.

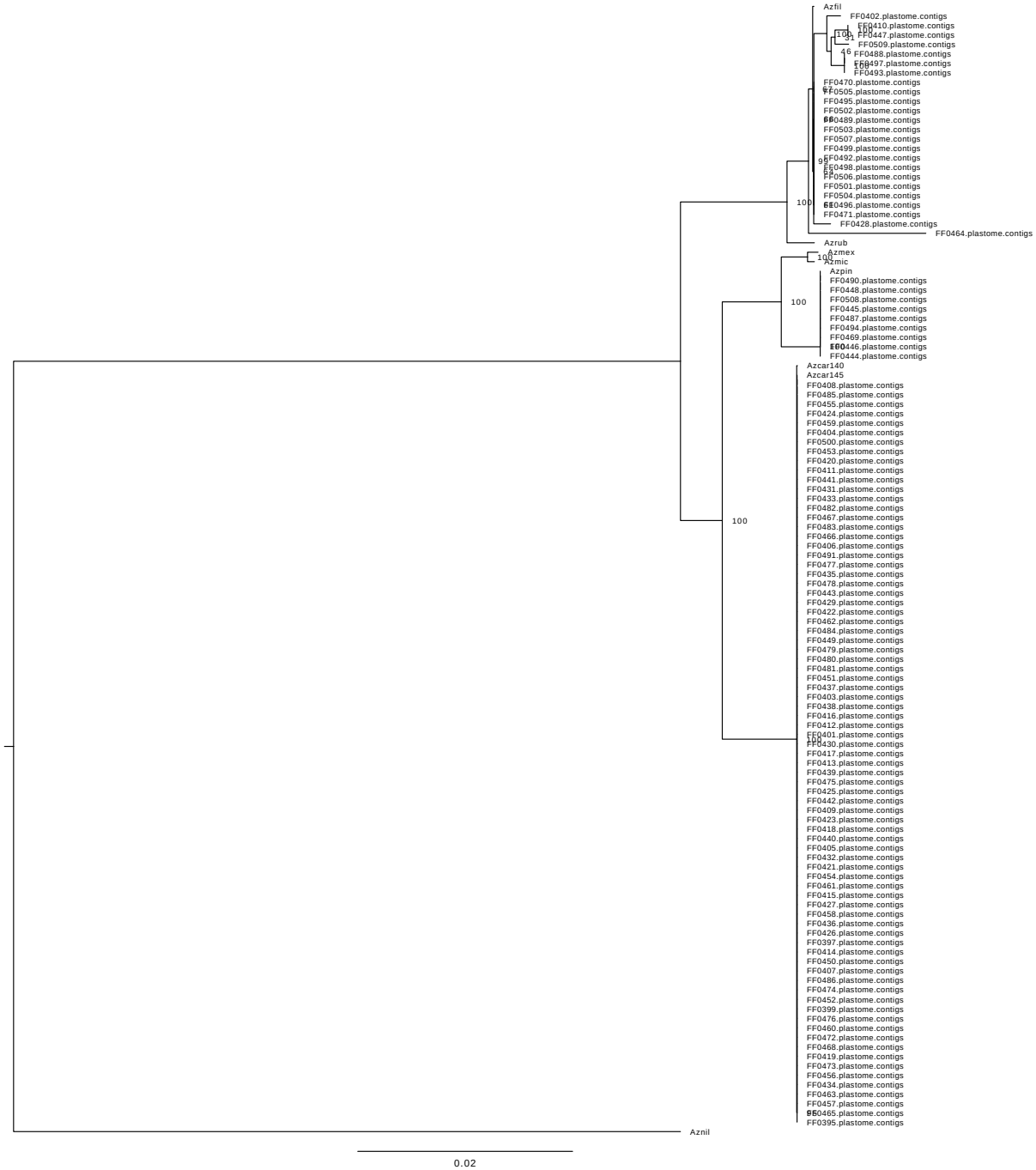

Supp. Fig. 1: Plastome phylogeny of *Azolla* samples with bootstrap values at nodes. The large clade is found to be similar to *A. caroliniana*, which is sister to a *A. microphyla/A. mexicana* clade (the *A. pinnata* chloroplast being a clear error in Genbank). These two clades are sister to an *A. filiculoides/ A. rubra* clade. These relationships reflect the current understanding of these taxa's evolutionary history.

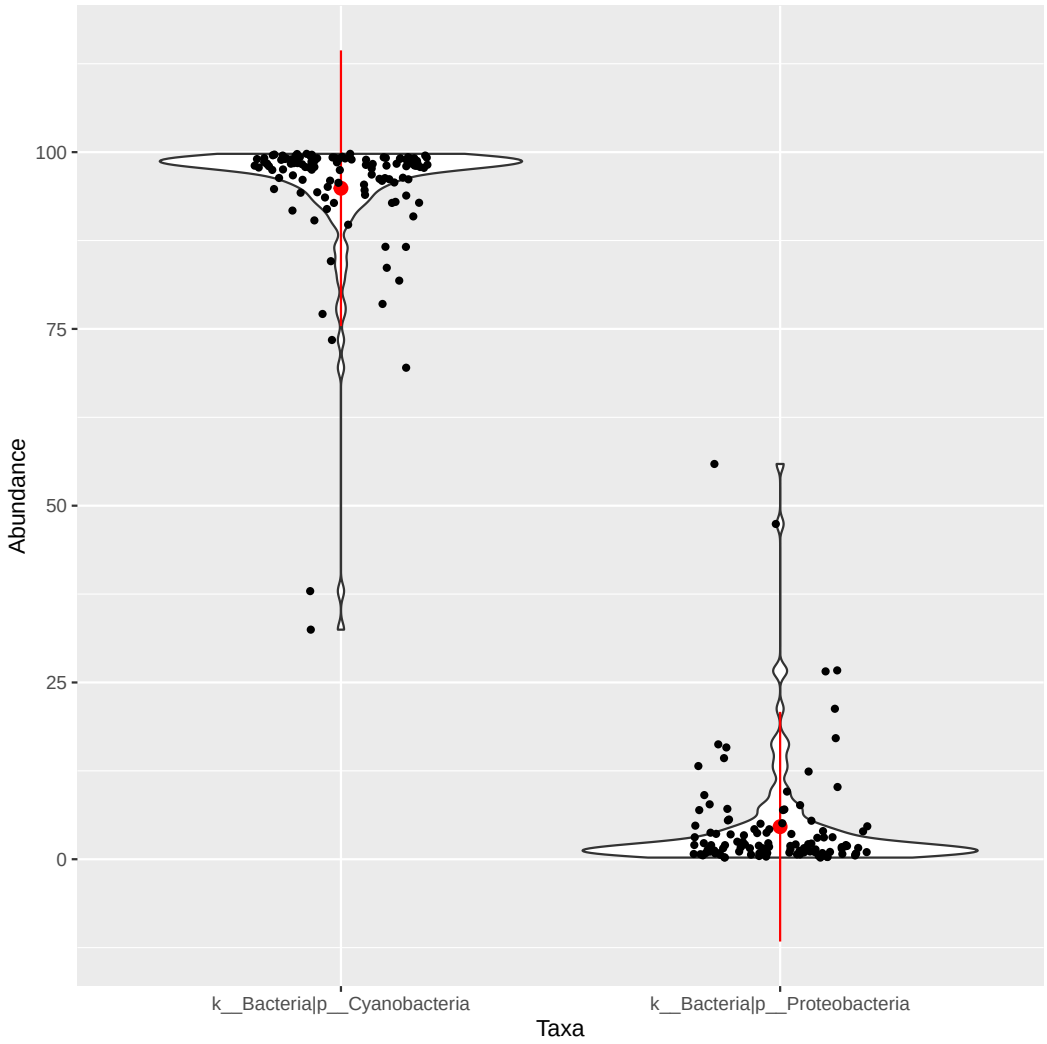

Supp. Fig. 2: Violin plots of the relative abundance of the two most abundant phyla across all samples with the mean and standard deviation in red.

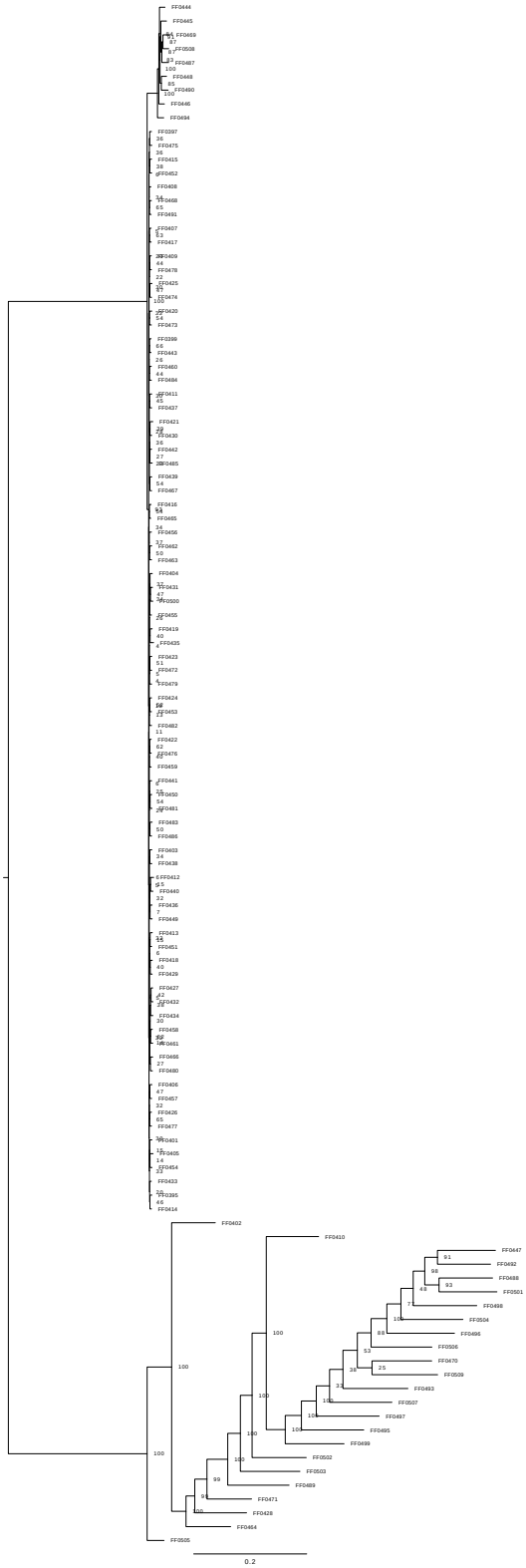

Supp. Fig. 3: ML phylogeny of *Azolla* samples inferred from SNP data with bootstrap values at nodes and branch length units in nucleotide substitutions per site.

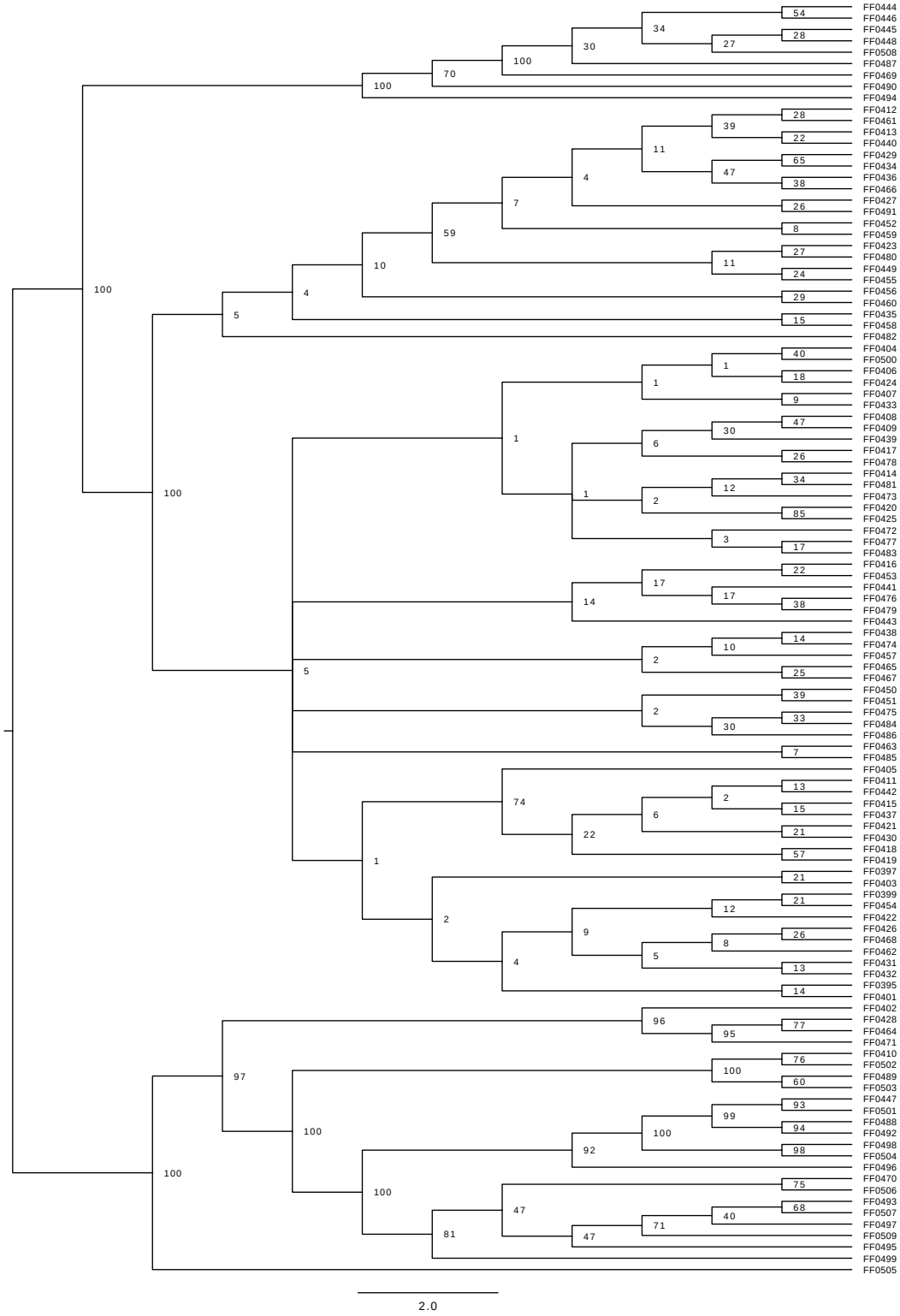

Supp. Fig. 4: Coalescent tree inferred using SVDQuartets with bootstrap values at nodes and branch lengths in coalescent units.

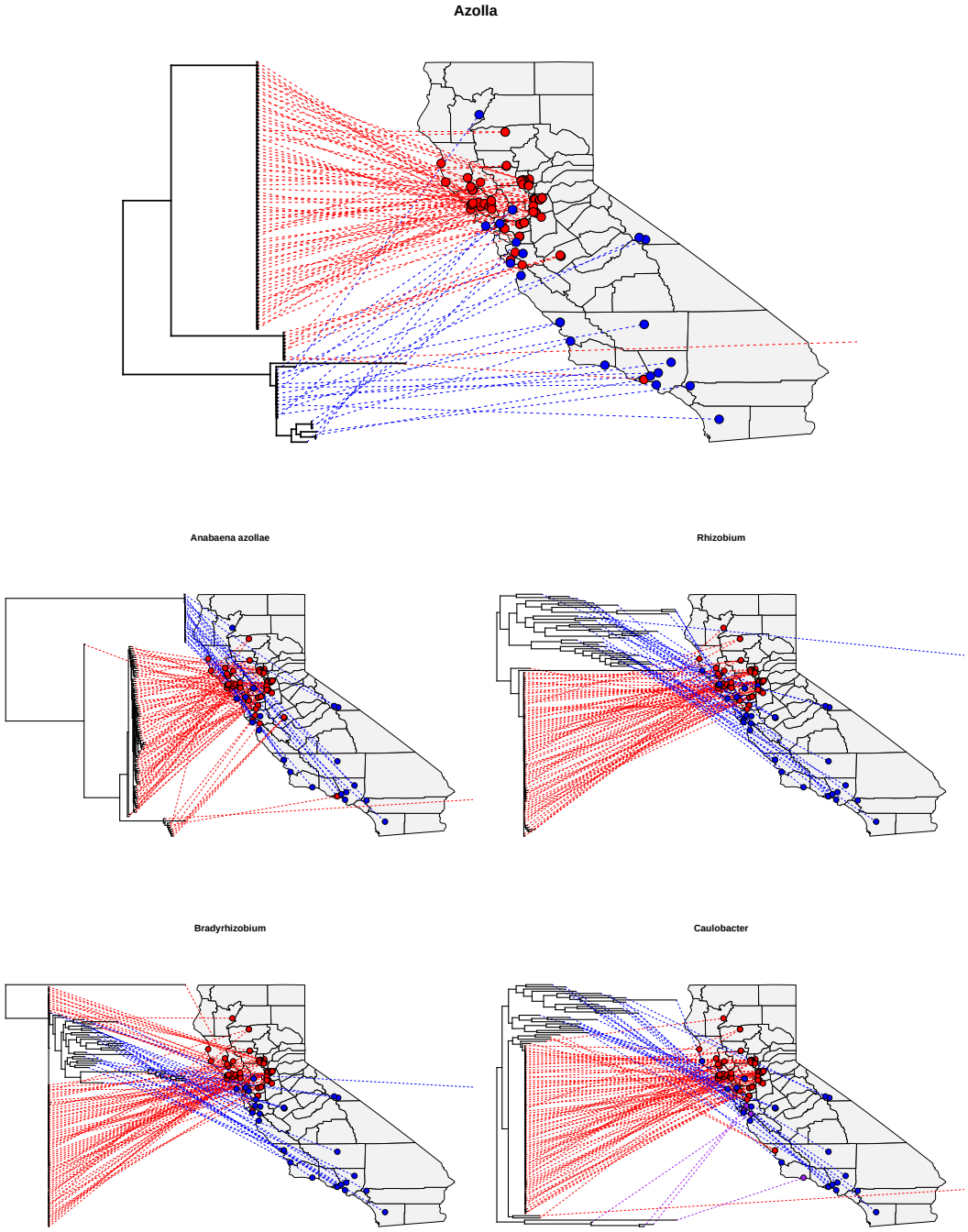

Supp. Fig. 5: Phylogenies of *Azolla* and its leaf pocket microbial taxa projected onto the samples' geographic location. Colors are broadly associated across trees to reflect potentially similar major groups in each taxa as well as to assist readability, although they should not be read as formal statements of co-diversification.

Supp. Tab. 1: Sample collection data

Sample name	Collection name	Geographic Location	Collection_date	Latitude and Longitude	Coverage
FF0395	F.Freund_293-14979	Spring Lake Park, Sonoma county, California	2021-Feb-10	38.45929, -122.65443	9.81336
FF0397	F.Freund_294-14980	Spring Lake Park, Sonoma county, California	2021-Feb-10	38.4512, -122.65347	8.61308
FF0399	F.Freund_295-14981	Laguna De Santa Rosa trail, Sonoma county, California	2021-Feb-12	38.41676, -122.8113	14.217
FF0401	F.Freund_296-14982	Riverside County Park, Sonoma county, California	2021-Feb-12	38.51644, -122.86393	11.4929
FF0402	F.Freund_292-14978	UC Berkeley, Alameda county, California	2021-Feb-05	37.874914, -122.238244	4.56492
FF0403	F.Freund_293-14979	Spring Lake Park, Sonoma county, California	2021-Feb-10	38.45929, -122.65443	7.88676
FF0404	F.Freund_294-14980	Spring Lake Park, Sonoma county, California	2021-Feb-10	38.4512, -122.65347	6.88168
FF0405	F.Freund_295-14981	Laguna De Santa Rosa trail, Sonoma county, California	2021-Feb-12	38.41676, -122.8113	7.10254
FF0406	F.Freund_296-14982	Riverside County Park, Sonoma county, California	2021-Feb-12	38.51644, -122.86393	9.19929
FF0407	F.Freund_297-14983	Cloverdale Riverfront Park, Sonoma county, California	2021-Feb-13	38.82603, -123.00664	9.32088
FF0408	F.Freund_298-14984	Cloverdale Riverfront Park, Sonoma county, California	2021-Feb-13	38.82293, -123.00974	9.96116
FF0409	F.Freund_299-14985	Cloverdale Riverfront Park, Sonoma county, California	2021-Feb-13	38.81849, -123.01181	11.0842
FF0410	F.Freund_300-14986	Audobon Canyon Ranch, Marin county, California	2021-Feb-16	37.9299, -122.68219	7.86395
FF0411	F.Freund_301-14987	Shadow Cliffs Regional Park, Alameda county, California	2021-Mar-02	37.66603, -121.83488	11.741
FF0412	F.Freund_302-14988	Shadow Cliffs Regional Park, Alameda county, California	2021-Mar-02	37.66691, -121.83823	44.3409
FF0413	F.Freund_303-14989	Shadow Cliffs Regional Park, Alameda county, California	2021-Mar-02	37.66814, -121.84361	25.2772
FF0414	F.Freund_304-14990	Contra Loma Regional Park, Contra Costa county, California	2021-Mar-04	37.97168, -121.82599	9.35674
FF0415	F.Freund_305-14991	Contra Loma Regional Park, Contra Costa county, California	2021-Mar-04	37.97356, -121.83136	8.94355
FF0416	F.Freund_306-14992	Contra Loma Regional Park, Contra Costa county, California	2021-Mar-04	37.97398, -121.8225	11.903
FF0417	F.Freund_307-14993	Cosumnes River Preserve, Sacramento county, California	2021-Mar-07	38.263732, -121.440121	7.97947
FF0418	F.Freund_308-14994	Cosumnes River Preserve, Sacramento county, California	2021-Mar-07	38.259844, -121.437601	8.79881
FF0419	F.Freund_309-14995	Cosumnes River Preserve, Sacramento county, California	2021-Mar-07	38.258056, -121.431826	7.69457
FF0420	F.Freund_310-14996	Cosumnes River Preserve, Sacramento county, California	2021-Mar-07	38.259191, -121.426778	7.45506
FF0421	F.Freund_311-14997	Cosumnes River Preserve, Sacramento county, California	2021-Mar-07	38.261154, -121.420542	10.9616
FF0422	F.Freund_312-14998	Cosumnes River Preserve, Sacramento county, California	2021-Mar-07	38.256748, -121.439148	10.5525
FF0423	F.Freund_313-14999	Sacramento National Wildlife Refuge, Glenn county, California	2021-Mar-09	39.42227, -122.16944	18.6806
FF0424	F.Freund_314-15000	Sacramento National Wildlife Refuge, Glenn county, California	2021-Mar-09	39.42213, -122.16398	9.64979
FF0425	F.Freund_315-15001	Sacramento National Wildlife Refuge, Glenn county, California	2021-Mar-09	39.43667, -122.16423	7.8067
FF0426	F.Freund_316-15002	Payne Creek BLM land, Tehama county, California	2021-Mar-09	40.27373, -122.19778	11.1772
FF0427	F.Freund_317-15003	Payne Creek BLM land, Tehama county, California	2021-Mar-10	40.27242, -122.19543	21.4705
FF0428	F.Freund_318-15004	Bucktail Hollow BLM land, Trinity county, California	2021-Mar-10	40.70494, -122.84583	6.14647
FF0429	F.Freund_319-15005	American River Parkway, Sacramento county, California	2021_Mar-22	38.60228, -121.48409	27.2787
FF0430	F.Freund_320-15006	Sutter's Landing Regional Park, Sacramento county, California	2021_Mar-22	38.58858, -121.4612	10.7989
FF0431	F.Freund_321-15007	Sutter's Landing Regional Park, Sacramento county, California	2021_Mar-22	38.5897, -121.45728	10.043
FF0432	F.Freund_322-15008	Sutter's Landing Regional Park, Sacramento county, California	2021_Mar-22	38.59023, -121.45422	12.8365
FF0433	F.Freund_323-15009	Sutter's Landing Regional Park, Sacramento county, California	2021_Mar-22	38.58936, -121.45016	10.2334
FF0434	F.Freund_324-15010	William B. Pond Regional Park, Sacramento county, California	2021_Mar-22	38.584, -121.34401	30.9599
FF0435	F.Freund_325-15011	William B. Pond Regional Park, Sacramento county, California	2021_Mar-22	38.58292, -121.33186	15.6081
FF0436	F.Freund_326-15012	William B. Pond Regional Park, Sacramento county, California	2021_Mar-22	38.58222, -121.33048	16.4053
FF0437	F.Freund_327-15013	William B. Pond Regional Park, Sacramento county, California	2021_Mar-22	38.58112, -121.33005	10.9599
FF0438	F.Freund_328-15014	William B. Pond Regional Park, Sacramento county, California	2021_Mar-22	38.5817, -121.3311	11.0392
FF0439	F.Freund_329-15015	William B. Pond Regional Park, Sacramento county, California	2021_Mar-22	38.58572, -121.33083	9.4962
FF0440	F.Freund_330-15016	Sunrise Recreation Area, Sacramento county, California	2021_Mar-22	38.63205, -121.27296	33.5765
FF0441	F.Freund_331-15017	Sunrise Recreation Area, Sacramento county, California	2021_Mar-22	38.62505, -121.28121	16.3836
FF0442	F.Freund_332-15018	Sunrise Recreation Area, Sacramento county, California	2021_Mar-22	38.62882, -121.27628	9.7094
FF0443	F.Freund_333-15019	Sunrise Recreation Area, Sacramento county, California	2021_Mar-22	38.62778, -121.2761	13.0143
FF0444	F.Freund_334-15020	San Luis National Wildlife Refuge, Merced county, California	2021-Mar-24	37.17493, -120.80167	9.17148
FF0445	F.Freund_335-15021	San Luis National Wildlife Refuge, Merced county, California	2021-Mar-24	37.17963, -120.81879	10.9122
FF0446	F.Freund_336-15022	San Luis National Wildlife Refuge, Merced county, California	2021-Mar-24	37.20137, -120.82523	7.77105
FF0447	F.Freund_337-15023	Malibu Creek State park, Los Angeles, California	2021-Mar-31	34.10312, -118.73864	14.5
FF0448	F.Freund_338-15024	Malibu Creek State park, Los Angeles, California	2021-Mar-31	34.09861, -118.73326	8.45417
FF0449	F.Freund_341-15025	MacKerricher State Park, Mendocino county, California	2021-Apr-14	39.4903, -123.79455	18.0248
FF0450	F.Freund_342-15026	Mill Creek road, Mendocino county, California	2021-Apr-14	39.12759, -123.12984	10.5229
FF0451	F.Freund_343-15027	Mill Creek road, Mendocino county, California	2021-Apr-14	39.13116, -123.13448	13.8941
FF0452	F.Freund_344-15028	Clear Lake State Park, Lake county, California	2021-Apr-14	39.01961, -122.81251	17.8488
FF0453	F.Freund_345-15029	Russian River, Mendocino county, California	2021-Apr-15	38.90751, -123.05816	9.28703
FF0454	F.Freund_346-15030	Nagasawa Community Park, Sonoma county, California	2021-Apr-15	38.48432, -122.71689	13.3198
FF0455	F.Freund_347-15031	Anadel State Park, Sonoma county, California	2021-Apr-16	38.40925, -122.59766	15.8904
FF0456	F.Freund_348-15032	Sugarloaf State Park, Sonoma county, California	2021-Apr-16	38.45018, -122.54028	14.7872
FF0457	F.Freund_349-15033	Sonoma Development Center, Sonoma county, California	2021-Apr-16	38.346185, -122.535045	12.5075
FF0458	F.Freund_350-15034	Tilden East Bay Regional Park , Alameda county, California	2021-May-03	37.896849, -122.249801	15.4308
FF0459	F.Freund_351-15035	Bodega Bay, Sonoma county, California	2021-May-06	38.33653, -123.05902	15.7808
FF0460	F.Freund_352-15036	Russian River, Sonoma county, California	2021-May-06	38.4649, -123.04729	14.1506
FF0461	F.Freund_353-15037	Russian River, Sonoma county, California	2021-May-06	38.46022, -123.05257	28.7906
FF0462	F.Freund_354-15038	Russian River, Sonoma county, California	2021-May-06	38.4669, -123.01187	10.6643
FF0463	F.Freund_355-15039	Russian River, Sonoma county, California	2021-May-06	38.49938, -122.9983	14.7847
FF0464	F.Freund_358-15041	Coyote Hills, Alameda county, California	2021-May-10	37.521642, -121.918585	5.22008
FF0465	F.Freund_359-15042	Sibley Volcanic Regional Preserve, Contra Costa county, California	2021-May-11	37.85937, -122.20583	7.82156
FF0466	F.Freund_360-15043	Big Break Regional Park, Contra Costa county, California	2021-May-28	38.00983, -121.72736	19.2938
FF0467	F.Freund_361-15044	Big Break Regional Park, Contra Costa county, California	2021-May-28	38.01221, -121.72827	12.5762
FF0468	F.Freund_362-15045	Big Break Regional Park, Contra Costa county, California	2021-May-28	38.00768, -121.72279	12.6423
FF0469	F.Freund_364-15046	Los Gatos City Park creek, Santa Clara county, California	2021-Jul-06	37.27298, -121.94801	8.21433
FF0470	F.Freund_366-15048	Laguna Park, Solano county, California	2021-Jul-30	38.32702, -122.0097	10.7304
FF0471	F.Freund_367-15049	Laguna Park, Solano county, California	2021-Jul-30	38.33517, -122.01347	5.12965
FF0472	F.Freund_368-15050	Feather River off Willson Rd., Sutter county, California	2021-Jul-30	39.01206, -121.60035	9.01463
FF0473	F.Freund_369-15051	Feather River off Willson Rd., Sutter county, California	2021-Jul-30	39.01146, -121.59948	8.35643
FF0474	F.Freund_370-15052	Feather River off Garden Hwy., Sutter county, California	2021-Jul-30	39.058, -121.61065	12.0956
FF0475	F.Freund_371-15053	Shanghai Bend Park, Sutter county, California	2021-Jul-30	39.09758, -121.59581	9.7154
FF0476	F.Freund_372-15054	Culvert on Ozwald Rd, Sutter county, California	2021-Jul-30	39.06889, -121.70841	15.6527
FF0477	F.Freund_374-15056	Levi on Hughes Rd., Sutter county, California	2021-Jul-30	39.07366, -121.74496	11.61
FF0478	F.Freund_375-15057	Hughes Rd., Sutter county, California	2021-Jul-30	39.07336, -121.74614	6.22105
FF0479	F.Freund_376-15058	Ozwald Rd., Sutter county, California	2021-Jul-30	39.06978, -121.78728	11.5675
FF0480	F.Freund_377-15059	Acme and Progress rd., Sutter county, California	2021-Jul-30	39.04421, -121.80074	15.7527
FF0481	F.Freund_378-15060	Reclamation rd., Sutter county, California	2021-Jul-30	38.96416, -121.7602	10.7168
FF0482	F.Freund_379-15061	Marcuse rd., Sutter county, California	2021-Jul-30	38.95254, -121.61932	15.6968
FF0483	F.Freund_380-15071	Stone Lake National Wildlife Refuge, Pond 1., Sacramento County, California	2021-Sept-20	38.37058, -121.49361	9.80097
FF0484	F.Freund_381-15072	Parker Slough, Stone Lakes National Wildlife Refuge., Sacramento County, California	2021-Sept-20	38.42707, -121.49921	11.1858
FF0485	F.Freund_382-15073	Snodgrass Slough, Twin Cities Rd., Sacramento County, California	2021-Sept-20	38.27668, -121.49536	12.058
FF0486	F.Freund_383-15074	Lake Lodi, San Joaquin County, California	2021-Sept-20	38.14939, -121.2966	12.7236
FF0487	Al Keuter_s.n. -14970	Quail Hollow Ranch County Park., Santa Cruz County, California	2021-Aug-16	37.082645, -122.062571	14.4974
FF0488	Al Keuter_s.n.2-14971	Thimman Greenhouse, University of California, Santa Cruz., Santa Cruz County, California	2021-Oct-1	36.99815702, -122.06219327	14.0945
FF0489	Beth Pearson_s.n. -14972	Cleveland National Forest., San Diego County, California	2021-May-24	33.106122, -116.86062	7.01314
FF0490	C.J.Rothfels_3479-6859	Flat River Impoundment, Durham County, North Carolina	2009-Sep-13	36.123, -78.826	8.54456
FF0491	C.J.Rothfels_4489-10078	Vicinity of Bobelaine Sanctuary, Sutter County, California	2014-Feb-05	38.93017, -121.60771	10.8109
FF0492	C.J.Rothfels_5437-14973	Hilltop Lake, Hilltop Lake Park, Richmond. Contra Costa County, California	2021-Jun-07	37.98697, -122.327583	14.0906
FF0493	C.J.Rothfels_5439-14968	Marina. Locke-Paddon Wetland Community Park, Monterey County, California	2021-Jul-07	36.691383, -121.802025	10.984
FF0494	C.J.Rothfels_5440-14969	Pinto Lake, N. end of. Watsonville., Santa Cruz County, California	2021-Jul-07	36.959763, -121.772933	5.9746
FF0495	David Keil_38123-14976	Santa Rita Ranch Preserve., San Luis Obispo County, California	2021-Jun-01	35.523981, -120.827494	9.80869
FF0496	David Keil_38202-1-14974	Santa Rita Ranch Preserve., San Luis Obispo County, California	2021-Jun-21	35.523981, -120.827494	12.7811
FF0497	David Keil_38286-14975	Black Lake Canyon., San Luis Obispo County, California	2021-Jun-15	35.055557, -120.566325	10.473
FF0498	Eric Cleveland_s.n. -14977	Ballona Freshwater Marsh., Los Angeles County, California	2021-Jun-30	33.966, -118.428	13.4723
FF0499	Ixchel Gonzalez Ramirez	Sequoia National Forest	2021-MAY-07	35.475097, -118.728447	9.57706
FF0500	Ixchel Gonzalez Ramirez_255-15062	Castello di amorosa winery., Napa County, California	2021-Jul-23	38.55848, -122.542149	5.64189
FF0501	Joshua Der_s.n. -15063	Owens River George., Mono County, California	2021-May-31	37.588254, -118.69506	13.697
FF0502	Joshua Der_s.n. -15064	Mammoth Lakes., Mono County, California	2021-Jul-05	37.641792, -118.854125	7.29138
FF0503	Matt_Guilliams_s.n.-6703	Santa Barbara Botanic Garden, Santa Barbara County, California	2021-Jun-6	34.456538, -119.710018	6.56854
FF0504	Mike Hundt_s.n. -15065	Basking Ridge Conservation Area., Santa Clara County, California	2021-May-15	37.242399, -121.75324	13.1312
FF0505	Mike Letteriello_1-15066	Palmdale, California., Kern County, California	2021-Apr-15	34.528065, -118.058212	3.59121
FF0506	Richard Rachman_1-15068	Hansen Dam Wildlife Preserve., Los Angeles County, California	2021-Apr-15	34.264779, -118.378582	11.5447
FF0507	Richard Rachman_2-15067	Pierce College., Los Angeles County, California	2021-Apr-15	34.182529, -118.575663	10.6588
FF0508	Roger Birkhead_s.n. -15069	Pomo Lake Park, Manchester., Mendocino County, California	2021-Jul-27	39.023809, -123.681963	10.6223
FF0509	Sonia Nosratinia_s.n. -15070	Santa Ana River., Riverside County, California	2021-May-15	33.941, -117.5847	10.5998

Supp. Tab. 2: Summary statistics for BugSeq metagenome assembly and taxonomic profiling

Sample Name	Abundance	N50 (Kbp)	Assembly Length (Kbp)	$\geq$ 20X	$\geq$ 50X	Median	Complete single copy BUSCOs
Anabaena azollae	53.6%	1079.5	5361.4	97.0%	97.0%	229.0X	119 (96%)
Root	32.9%	26.0	39736.7				NA
Rhizobium	1.7%	451.8	4245.0				112 (90.3%)
Bradyrhizobium	0.2%	21.5	1384.2				18 (14.5%)
Caulobacter	0.2%	22.9	960.9				42 (33.9%)
Rhizobiaceae	0.2%	304.0	516.0				9 (7.3%)
Alphaproteobacteria	0.0%	29.7	193.1				0
Ascomycota	0.0%	11.4	11.4				NA
Bosea	0.0%	8.1	8.1				0
Chachezhania	0.0%	10.0	10.0				0
Costertonia	0.0%	12.1	12.1				0
Dyadobacter	0.0%	7.1	7.1				0
Fusarium	0.0%	9.1	9.1				NA
Ginsengibacter	0.0%	11.2	11.2				0
Hoeflea	0.0%	12.2	12.2				1 (0.8%)
Kinneretia	0.0%	7.6	7.6				0
Maribacter	0.0%	8.5	8.5				0
Methylibium	0.0%	7.4	7.4				1 (0.8%)
Mucilaginibacter	0.0%	10.2	73.7				0
Pandoraea soli	0.0%	8.1	8.1			0.0X	0
Pedobacter	0.0%	8.7	70.5				2 (1.6%)
Pirellula	0.0%	8.4	8.4				0
Pseudomonadota	0.0%	43.4	52.9				0
Pseudoxanthomonas	0.0%	9.1	9.1				0
Reyranella	0.0%	9.1	9.1				1 (0.8%)
Rhodopseudomonas	0.0%	8.8	8.8				0
Rhodospirillales	0.0%	13.9	51.6				1 (0.8%)
Tardiphaga	0.0%	14.5	14.5				0
Trichoderma	0.0%	9.6	18.9				NA
Undibacter	0.0%	7.2	7.2				0

Supp. Tab. 3: Statistical tests of codiversification ("cospeciation" in phytools and "parafit" in ape) between two trees based on tree distance. The tests run in the package "cospeciation" were performed for both RF and SPR distances and p-values calculated either by simulation of pure-birth trees (simulation) or permutation of tip labels on a fixed tree (permutation). The number of simulations or permutations for each test: n=500. For the parafit global test, 999 permutations were performed for each test. The null hypothesis for all tests is that there are no similarity between trees.

Tree 1	Tree 2	RF distance permutation, Mean (SD) from null, p-value	RF distance simulation, Mean (SD) from null, p-value	SPR distance permutation, Mean (SD) from null, p-value	SPR distance simulation, Mean (SD) from null, p-value	ParaFitGlobal test statistic, p-value	Tests significant
Azolla nuc. tree	*Anabaena azollae*	206, 217.7 (0.8), 0.001996	206, 216.2 (1.8), 0.001996	46, 51.2 (1.1), 0.001996	46, 51.1 (1.2), 0.003992	24.05071, 0.01	5/5
Azolla nuc. tree	*Rhizobium*	218, 217.7 (0.8), 1	218, 216.5 (1.6), 1	50, 51.1 (1.3), 0.326733	50, 51.6 (1), 0.138614	7.991151, 0.555	0/5
Azolla nuc. tree	*Caulobacter*	216, 217.6 (0.8), 0.165669	216, 216.4 (1.6), 0.582834	40, 50.7 (1.3), 0.0499	48, 51.3(1.1), 0.005988	4.79612, 0.735	2/5
Azolla nuc. tree	*Bradyrhizobium*	214, 217.6 (0.9), 0.021956	214, 214.9 (2.4), 0.457086	49, 51 (1.2), 0.103792	49, 50.9 (1.2), 0.0998	26.48987, 0.001	2/5
Anabaena azollae	*Caulobacter*	214, 217.7 (0.8), 0.011976	214, 215.1 (2.3), 0.437126	49, 50 (1.4), 0.325349	49, 50.6 (1.2), 0.181637	17.21153, 0.001	2/5
Anabaena azollae	*Bradyrhizobium*	212, 217.7 (0.8), 0.001996	212, 214.8 (2.4), 0.223553	48, 50.3 (1.3), 0.091816	48, 50.2 (1.3), 0.093812	32.66356, 0.133	1/5
Anabaena azollae	*Rhizobium*	216, 217.7 (0.7), 0.127745	216, 215.5 (2.1), 0.742515	50, 50.4 (1.4), 0.51497	50, 50.6 (1.2), 0.461078	28.72107, 0.001	1/5
Bradyrhizobium	*Caulobacter*	196, 217.7 (0.7), 0.001996	196, 213.3 (2.9), 0.001996	44, 50 (1.4), 0.001996	43, 49.6 (1.4), 0.001996	36.28696, 0.312	4/5
Bradyrhizobium	*Rhizobium*	204, 217.8 (0.6), 0.001996	204, 213 (3), 0.011976	48, 50.3 (1.4), 0.111776	48, 49.5 (1.3), 0.193613	55.31025, 0.233	2/5
Caulobacter	*Rhizobium*	217, 217.7 (0.7), 0.001996	192, 211.7 (3.4), 0.001996	43, 50.1 (1.4), 0.001996	43, 49 (1.3), 0.001996	18.60991, 0.002	5/5
Azolla SVDQ tree	*Anabaena azollae*	200, 217.5 (1), 0.001996	200, 213.6(2.9), 0.001996	47, 51.6 (1.1), 0.001996	47, 49.9 (1.3), 0.02994	67868.59, 0.001	5/5
Azolla SVDQ tree	*Rhizobium*	216, 217.7 (0.8), 0.141717	216, 214.9 (2.2), 0.832335	49, 51.6 (1.1), 0.031936	49, 50.7 (1.1), 0.137725	24971.56, 0.001	2/5
Azolla SVDQ tree	*Caulobacter*	218, 217.6 (0.9), 1	218, 215.4 (2.2), 1	51, 51.1 (1.2), 0.592814	51, 50.6 (1.2), 0.776447	16085.25, 0.001	1/5
Azolla SVDQ tree	*Bradyrhizobium*	216, 217.6 (0.9), 0.201597	216, 215.1 (2.2), 0.818363	48, 51.5 (1.1), 0.011976	48, 50.6 (1.2), 0.0499	39594.57, 0.052	3/5
Azolla plastome tree	*Anabaena azollae*	206, 218 (0.2), 0.001996	206, 216.2 (1.8), 0.001996	39, 41.9 (1.9), 0.103792	39, 51.2 (1.1), 0.001996	0.02433967, 0.005	4/5
Azolla plastome tree	*Rhizobium*	216, 217.9 (0.3), 0.027944	216, 216 (1.8), 0.668663	39, 41.6 (2), 0.135729	39, 51.2 (1.1), 0.001996	0.01266035, 0.31	4/5
Azolla plastome tree	*Caulobacter*	216, 217.9 (0.4), 0.027944	215, 215.7 (2), 0.702595	37, 41.4 (2), 0.037924	37, 50.9 (1.1), 0.001996	0.007746964, 0.694	3/5
Azolla plastome treee	*Bradyrhizobium*	218, 217.9 (0.4), 1	218, 216.2 (1.7), 1	38, 41.7 (2), 0.045908	38, 51.1 (1.1), 0.001996	0.02544839, 0.664	2/5